J. Fluid Mech. (1989), *vol.* 209, *pp.* 35–55
Printed in Great Britain

The interaction between swirling and recirculating velocity components in unsteady, inviscid flow

By P. A. DAVIDSON

Department of Applied Mathematics and Theoretical Physics, University of Cambridge, Silver Street, Cambridge CB3 9EW, UK†

(Received 25 September 1987 and in revised form 16 March 1989)

In this paper we consider the transient evolution of a swirling, recirculating flow in a truncated cylinder. In particular, we consider an initial time period during which the evolution of the flow is controlled by inertia. Such flows exhibit a mutual interaction between the swirl and the poloidal recirculation, whereby any axial gradient in swirl alters the recirculation, which, in turn, redistributes the swirl. This interaction may be visualized as a flexing of the poloidal vortex lines, the best known example of which is the inertial wave. Physical arguments and numerical experiments suggest that, typically, a strong, oscillatory recirculation will develop. We examine the exchange of energy between the swirl and recirculation, and show that the direction of transfer depends on the relative signs of ψ and $\partial u_\theta/\partial z$. In addition, there is a limit to the amount of energy that may be exchanged, since conservation of angular momentum imposes a lower bound on the kinetic energy of the swirl. The characteristic reversal time for the recirculation is estimated by considering the history of fluid particles on the endwalls. Its magnitude depends on the relative strengths of the swirl and recirculation. When the recirculation is large, the reversal time exceeds the turn-over time for a poloidal eddy and, consequently, the vortex lines accumulate at the stagnation points on the endwalls. This leads to accelerated local diffusion on the axis. An elementary one-parameter model is proposed for these nonlinear oscillations. In the limit of very weak recirculation, this model is consistent with the exact solution for inertial waves, while for strong recirculation, it confirms that the reversal time is greater than the turn-over time, and that the vortex lines accumulate on the axis.

1. Introduction

Suppose that we have a cylinder in which, at time $t = 0$, fluid is given a non-uniform swirl distribution. This could be achieved by, say, the impulsive action of a body force. What occurs subsequently? Ultimately, of course, the fluid is brought to rest by the action of viscosity. However, we shall show that there is a time period during which shear is ineffective, and yet the flow field exhibits some interesting features, such as a strong, oscillatory recirculation.

There are many industrial processes involving swirling fluid, and a number of these occur in cylindrical containers. Stirred chemical mixing vessels, cyclone separators, combustion systems and the magnetic stirring of molten metals are just a few examples. While there have been many detailed numerical and experimental studies of such flows (see Gupta, Lilley & Syred 1984), theoretical analyses tend to fall into

† Present address: Westinghouse Research and Development Center, 1310 Beulah Road, Pittsburgh, PA 15235, USA.

one of six categories: (i) flows that consist of a small perturbation about a state of rigid-body rotation, such as inertial waves (see Greenspan 1968); (ii) steady flows involving relative rotation between a viscous fluid and one or more discs, with or without cylindrical sidewalls (Batchelor 1951; Greenspan 1968; Dijkstra & van Heijst 1983, and many others); (iii) vortex breakdown (Hall 1967 gives a review); (iv) steady, axisymmetric, inviscid flows in which the distribution of energy and angular momentum between streamlines may be specified at some upstream point (see Batchelor 1967 for a general discussion and Bloor & Ingham 1987 for its application to cyclone separators); (v) centrifugal instabilities and Taylor vortices (see, for example, Howard & Gupta 1962 and Drazin & Reid 1981); (vi) steady, viscous, concentrated vortex cores (Lewellen 1962 and Hall 1967).

One class of flows which have not been studied extensively are unsteady, inviscid, swirl flows with a strong recirculation. These involve a complex interaction between the swirl and the recirculation and it is this which is the subject of the present paper. Such flows are relevant to, for example, the electromagnetic stirring of molten metal.

Electromagnetic stirring is a widespread industrial process whereby molten metal is homogenized by the application of a rotating magnetic field. This field induces an azimuthal body force which, in turn, produces swirl in the melt (Davidson & Hunt 1987). One recent trend has been to apply the magnetic body force in an intermittent fashion, whereby the melt is spun up first in one direction and then in the other. Between successive reversals in the body force there is a dormant period, during which the melt is allowed to spin under the action of its own inertia (Kojima *et al.* 1983). In such cases it is important to know whether a secondary recirculation develops, as this dominates the mixing processes within the melt.

Typically, the dormant period t between successive applications of the body force is of the order of 5 s. Also, the characteristic rotation rate Ω is ~ 10 rad/s and the Reynolds number $\mathbb{R}$ is $\sim 10^5$. It follows that, in this case,

$$1 \ll \Omega t \ll \mathbb{R}^{\frac{1}{2}}.$$

We shall see that this inequality implies that the unforced flow field undergoes a substantial evolution, involving a strong, oscillatory recirculation, and that this process is dominated by inertia, rather than shear stresses.

In this paper we restrict ourselves to axisymmetric, inviscid flow in a cylinder of radius R and length l. (For simplicity, we shall take R and l to be of the same order.) The assumption that the flow is inviscid is highly restrictive, since viscosity plays a crucial role in the later stages of the evolution of a swirling flow. We must estimate at what stage viscosity becomes important.

There are at least three mechanisms by which viscosity ultimately establishes control of the flow. In the first instance, von Kármán boundary layers are established on the endwalls, producing a recirculation with a timescale (see Greenspan 1968) of

$$\tau_\nu \sim l/(\nu\Omega)^{\frac{1}{2}}.$$

Simultaneously, a concentrated vortex core starts to form on the axis as the secondary flow tries to advect a non-zero angular momentum, $\Gamma = u_\theta r$, onto the centreline. This process is controlled by the stagnation points on the endwalls. We shall consider this in more detail in §5. It is shown there that the diffusion timescale in these vortex cores is

$$\tau_\nu \sim \frac{l^2}{\nu}(\Omega\tau_t)^2\,|\ln(\Omega\tau_t)|, \quad \Omega\tau_t \ll 1,$$

where τ_t is the 'turn-over time' for the poloidal recirculation.

Finally, slow diffusion between streamlines tends to eliminate gradients in angular momentum Γ and azimuthal vorticity ω_θ/r (Batchelor 1956). This occurs on a timescale

$$\tau_\nu \sim l^2/\nu.$$

Typically, the fluid viscosity is small, and consequently, the smallest of these three diffusion timescales is usually the first, determined by the von Kármán boundary layers. Consequently, we shall restrict attention to the time period,

$$\Omega t \ll \mathbb{R}^{\frac{1}{2}}, \quad \text{where } \mathbb{R} = \Omega R^2/\nu.$$

We may then neglect the action of viscosity on the flow, except in the boundary layers immediately adjacent to the walls.

2. The governing equations of motion and the coupling of the azimuthal and poloidal velocity fields

We shall use a cylindrical polar coordinate system (r, θ, z), where $r \leqslant R$ and $0 \leqslant z \leqslant l$. It is convenient to separate the velocity $\boldsymbol{u}$ and vorticity $\boldsymbol{\omega}$ into azimuthal and poloidal components and examine the interaction between them. Thus $\boldsymbol{u}_\theta$, or $\boldsymbol{\omega}_\mathrm{p} = \boldsymbol{\nabla} \times \boldsymbol{u}_\theta$, represents the swirling motion, while $\boldsymbol{u}_\mathrm{p}$, or $\boldsymbol{\omega}_\theta = \boldsymbol{\nabla} \times \boldsymbol{u}_\mathrm{p}$, represents motion in the (r, z)-plane.

For axisymmetric flow, we may introduce the Stokes stream function ψ, defined by

$$\boldsymbol{u}_\mathrm{p} = \boldsymbol{\nabla} \times [(\psi/r)\, \hat{\boldsymbol{e}}_\theta].$$

Noting that $\boldsymbol{\omega}_\mathrm{p} = \boldsymbol{\nabla} \times \boldsymbol{u}_\theta$, we see that the angular momentum, $\Gamma = u_\theta r$, is the stream function for the poloidal vorticity.

The equations of motion for inviscid, swirling flow may be written in the form

$$\frac{\mathrm{D}\Gamma}{\mathrm{D}t} = 0, \tag{1}$$

$$\frac{\mathrm{D}}{\mathrm{D}t}\left(\frac{\omega_\theta}{r}\right) = \frac{\partial}{\partial z}\left(\frac{\Gamma^2}{r^4}\right). \tag{2}$$

The quantity ω_θ/r will appear frequently. From Stokes' theorem, the integral of ω_θ/r throughout any (axisymmetric) volume V is related to the circulation around its bounding curve C in the (r, z)-plane. In particular,

$$\int_V (\omega_\theta/r)\, \mathrm{d}V = 2\pi \oint_C \boldsymbol{u}_\mathrm{p} \cdot \mathrm{d}\boldsymbol{r}. \tag{3}$$

Equations (1) and (2) show the mutual interaction between the swirling flow, represented by Γ, and the recirculation, represented by ω_θ/r. Any axial gradient in swirl acts as a source of poloidal recirculation, which, in turn, redistributes Γ. This interplay has been extensively explored in the case of steady, viscous flows (see, for example, Hall 1967), and we shall be concerned here with its consequences in unsteady, inviscid flow.

Note that (1) is a direct consequence of Kelvin's circulation theorem, and may be generalized to give

$$\frac{\mathrm{D}}{\mathrm{D}t} f(\Gamma) = 0, \tag{4}$$

where f is an arbitrary function of Γ. We shall use this in §6.

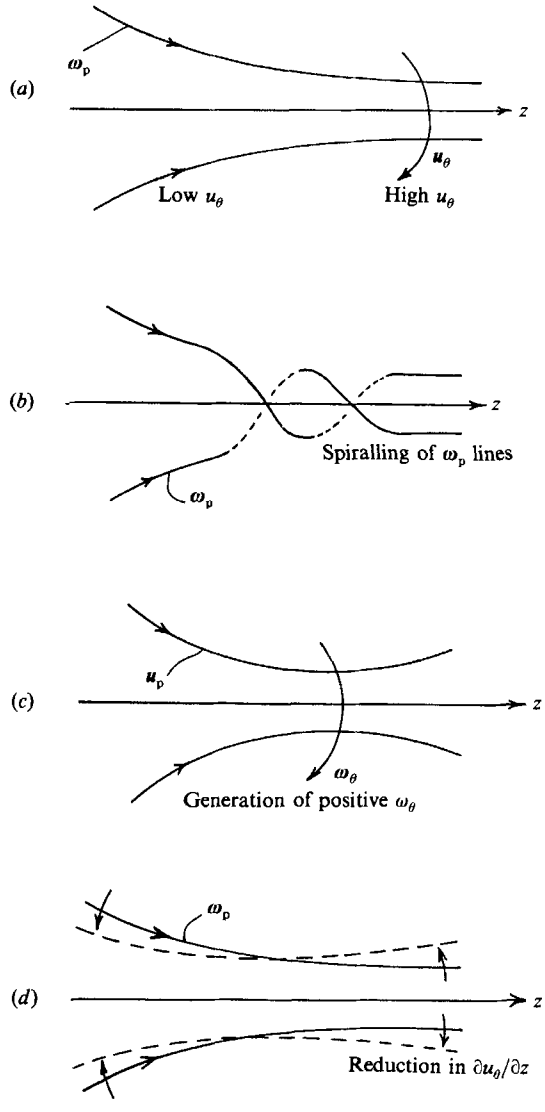

FIGURE 1. Generation of azimuthal vorticity ω_θ by spiralling of the $\boldsymbol{\omega}_p$ lines; and consequent advection of the $\boldsymbol{\omega}_p$ lines.

The source term in (2) may be rewritten as $|\nabla \times (\boldsymbol{u}_\theta \times \boldsymbol{\omega}_p)|$, representing a spiralling of the poloidal vortex lines by $\boldsymbol{u}_\theta$. This is the mechanism by which the swirl generates azimuthal vorticity, and the process is illustrated in figures 1 (*a*) and 1 (*b*). Note that differential rotation is required for this, as otherwise the $\boldsymbol{\omega}_p$ lines lie parallel to the axis and rotate without distortion.

Now suppose that at time $t = 0$, we have a positive axial gradient in swirl, but no recirculation, as shown in figure 1 (*a*). Then a positive value of ω_θ will be swept out, as described above. This is consistent with (2) and is associated with the poloidal velocity field $\boldsymbol{u}_p$ shown in figure 1 (*c*). This poloidal velocity will, in turn, advect the poloidal vortex lines in accordance with (1), since Γ is the stream function for $\boldsymbol{\omega}_p$. The result is a tilting of the $\boldsymbol{\omega}_p$ lines as shown in figure 1 (*d*), causing a reduction in the axial gradient of u_θ.

However, as a result of the inertia of the fluid, the advection of the ω_p lines will persist, even after the axial gradient in u_θ is eliminated. The result will be a reversal in the gradient of the ω_p lines, associated with a negative value of $\partial u_\theta/\partial z$. This, in turn, will force a reduction in ω_θ in accordance with (2), and the entire process is then reversed.

This sequence of events provides a physical mechanism by which oscillations may occur. These may be visualized as a 'flexing' of the poloidal vortex lines, and one manifestation of this is the inertial wave, which is a small-amplitude oscillation that may be superimposed on any z-independent swirl flow, $u_\theta = V(r)$. (See, for example, Drazin & Reid 1981.)

To investigate possible oscillations, we must look at the second-order convective derivative of ω_θ. From (2) we may show that

$$\frac{\mathrm{D}^2}{\mathrm{D}t^2}\left(\frac{\omega_\theta}{r}\right) - J\frac{\mathrm{D}}{\mathrm{D}t}\left(\frac{\omega_\theta}{r}\right) + \Phi\left[\frac{\omega_\theta}{r} + \frac{1}{r}\frac{\partial u_z}{\partial r}\right] = 0,$$

where $\Phi = (1/r^3)(\partial \Gamma^2/\partial r)$ is Rayleigh's discriminant, and $J = r^3(\partial/\partial r)(u_r/r^3)$.

In the case of inertial waves, we may linearize this about the base flow $u_\theta = V(r)$ to give the well-known equation

$$\frac{\partial^2}{\partial t^2}\left(\frac{\omega_\theta}{r}\right) + \Phi(r)\left[\frac{\omega_\theta}{r} + \frac{1}{r}\frac{\partial u_z}{\partial r}\right] = 0. \tag{5}$$

This may be solved to give the natural frequencies and normal modes of the standing waves, the former being of the order of $\Phi^{\frac{1}{2}}$. Note that Rayleigh's criterion for stable axisymmetric oscillations is $\Phi \geqslant 0$.

These inertial waves cannot readily be interpreted in terms of the Coriolis force, except for the case of rigid-body rotation. However, they may be visualized as the oscillation of otherwise parallel poloidal vortex lines, as described above.

3. Numerical simulation of a swirling flow

In order to illustrate the comments of the preceding section, it is useful to consider the following numerical experiment. Suppose that, at time $t = 0$, we specify a non-uniform swirl distribution, given by, say,

$$\Gamma = \Omega r^2\{1 + \tfrac{1}{2}[1 - (r/R)^2]\cos(\pi z/l)\}, \tag{6}$$

where Ω is a constant. In addition, we shall take the initial recirculation $\boldsymbol{u}_p$ to be zero.

We shall follow the evolution of this flow using a finite-difference code, described in Davidson & Hunt (1987). This code solves the Navier–Stokes equations, subject to the no-slip boundary condition, using a quadratic upwind interpolation scheme. The Reynolds number was set at 10^6, although, in practice, any specified viscosity is inevitably augmented by 'numerical diffusion'. The parameters Ω, R and l were given values of 1 rad/s, 1 m and 2 m respectively. No special effort was made to maintain accuracy in the boundary layers as the primary interest was in the initial, inviscid flow.

Figure 2(*a*) shows the poloidal recirculation at times $t = 2$, 6 and 10 s. Clearly, the poloidal eddy oscillates back and forth, ω_θ being first negative, then positive and then negative again. The time required for each reversal of the eddy is $\tau_r = 4.1$ s, and the maximum magnitude of $\boldsymbol{u}_p$ is approximately 0.29 m/s. Thus the recirculation is of the same order as the initial swirl.

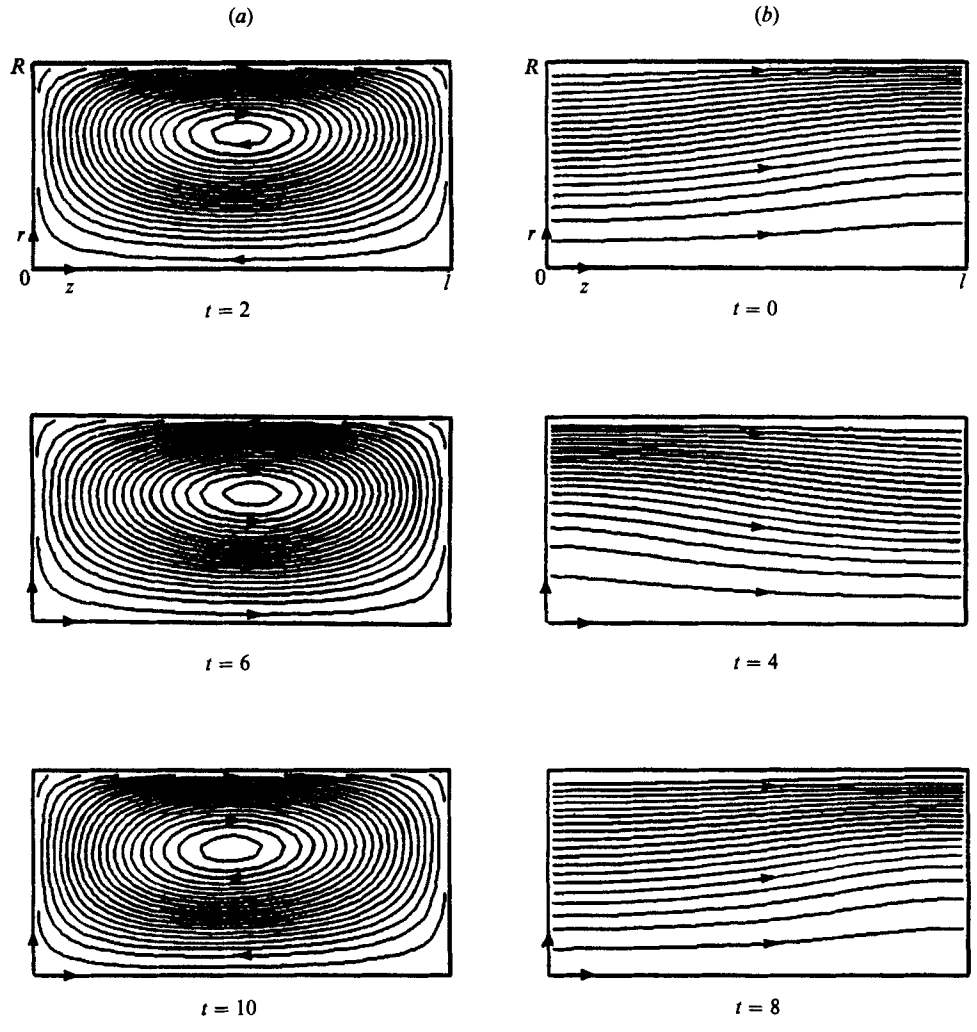

FIGURE 2. Computed evolution of a swirling flow. (*a*) Poloidal recirculation at $t = 2$, 6 and 10 s. (*b*) Poloidal vortex lines at $t = 0$, 4 and 8 s.

As the recirculation oscillates back and forth, it carries with it the angular momentum Γ. This may be illustrated by examining contours of constant Γ, that is, the poloidal vortex lines. These are shown in figure 2(*b*) for times $t = 0$, 4, and 8 s. The ω_p lines are successively compressed at either end of the cylinder, depending on the sign of ω_θ. We shall discuss this in more detail in §5, where the computations are compared with a simple analytical model of the oscillations.

Figure 3 shows the flow generated by the initial swirl distribution,

$$\Gamma = \Omega r^2\{1+[1-(r/R)^2]\cos(\pi z/l)\}. \tag{7}$$

In this case the initial gradient in swirl is larger, and consequently the induced recirculation is stronger. Here the reversal time is $\tau_r = 4.4$ s, and the maximum magnitude of $\boldsymbol{u}_p$ is approximately 0.50 m/s.

Note that, in cases where the initial recirculation is zero, such as that above, we

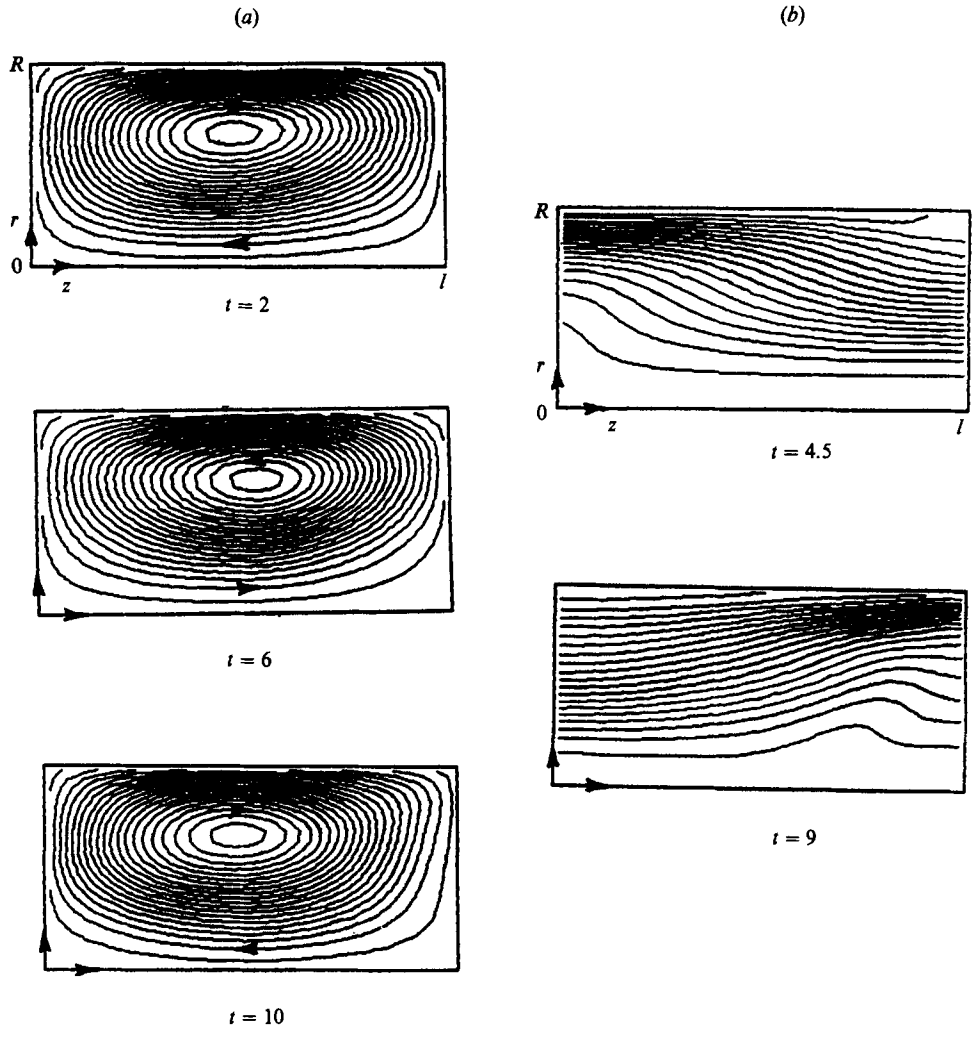

FIGURE 3. Numerical experiment of swirling flow with stronger recirculation. (Initial conditions given by (7).) (*a*) Poloidal recirculation, (*b*) poloidal vortex lines.

may calculate the early growth of the poloidal eddy exactly. For small t, (2) may be linearized to give

$$\frac{\omega_\theta}{r} = \frac{t}{r^4}\frac{\partial \Gamma_0^2}{\partial z},$$

where Γ_0 is the initial distribution of Γ. This gives

$$\nabla^2\psi - \frac{2}{r}\frac{\partial \psi}{\partial r} = -r\omega_\theta = -\frac{t}{r^2}\frac{\partial \Gamma_0^2}{\partial z}, \tag{8}$$

from which ψ may be calculated.

The problem of predicting the evolution of such a flow for periods greater than Ω^{-1} is that the nonlinear form of (1) and (2) precludes the development of an exact analytical solution. Consequently, we shall look at the integral properties of these flows, to determine what global constraints this places on their evolution.

4. Integral properties of the flow

4.1. *Conservation of angular momentum and kinetic energy*

Equation (1) shows that Γ, the angular momentum, is a materially conserved quantity. Let I_Γ be the volume integral of Γ throughout the flow field,

$$I_\Gamma = \int_V \Gamma \, \mathrm{d}V. \tag{9}$$

Then (1) implies

$$\frac{\mathrm{d}}{\mathrm{d}t} I_\Gamma = 0. \tag{10}$$

More generally, (4) shows that

$$\frac{\mathrm{d}}{\mathrm{d}t} \int_V f(\Gamma) \, \mathrm{d}V = 0. \tag{11}$$

Another integral invariant is the total kinetic energy per unit mass,

$$E = \int_V \tfrac{1}{2} u^2 \, \mathrm{d}V.$$

It is instructive to divide E into E_θ and E_p, the kinetic energies of the azimuthal and poloidal velocity fields

$$E_\theta = \int_V \tfrac{1}{2} u_\theta^2 \, \mathrm{d}V,$$

$$E_\mathrm{p} = \int_V \tfrac{1}{2} u_\mathrm{p}^2 \, \mathrm{d}V = \int_V \tfrac{1}{2} \psi (\omega_\theta / r) \, \mathrm{d}V.$$

(The latter equality follows from the application of the divergence theorem to $\nabla \cdot [(\psi/r)\, \hat{\boldsymbol{e}}_\theta \times \boldsymbol{u}_\mathrm{p}]$, while noting that $\psi = 0$ on the boundary.) Conservation of energy now requires

$$\frac{\mathrm{d}}{\mathrm{d}t} [E_\theta + E_\mathrm{p}] = 0.$$

We shall consider the exchange of kinetic energy between the azimuthal and poloidal velocity fields. Noting that $\psi = 0$ on the boundary, we may use (1) to show

$$\frac{\mathrm{d}}{\mathrm{d}t} E_\mathrm{p} = -\frac{\mathrm{d}}{\mathrm{d}t} E_\theta = \int_V \left\{ \frac{u_\theta^2}{r} \right\} u_r \, \mathrm{d}V = \int_V \frac{\psi}{r} \frac{\partial}{\partial z} \left\{ \frac{u_\theta^2}{r} \right\} \mathrm{d}V. \tag{12}$$

Physically, this represents the work done by the poloidal velocity field in moving a fluid element radially outwards against the pressure gradient set up by the centripetal acceleration. Note that there is no transfer of energy between the two velocity fields when the axial gradient in Γ is zero. This is consistent with the source term in (2) being zero. In general, the direction of transfer of energy depends on the relative signs of ψ and $\partial \Gamma^2 / \partial z$. In the example given in §3, ψ and $\partial \Gamma^2 / \partial z$ are initially of the same sign, so that kinetic energy is transferred to the poloidal velocity field.

Conservation of angular momentum imposes a limitation on the amount of energy which may be transferred from $\boldsymbol{u}_\theta$ to $\boldsymbol{u}_\mathrm{p}$. This may be shown by applying Schwarz's integral inequality to I_Γ

$$\left(\int_V \Gamma \, \mathrm{d}V \right)^2 \leqslant \int_V u_\theta^2 \, \mathrm{d}V \int_V r^2 \, \mathrm{d}V.$$

Let $V = \pi R^2 l$, the volume of the flow field. Then, from the expression above,

$$E_\theta \geqslant \frac{I_\Gamma^2}{R^2 V}. \tag{13}$$

The equality holds if, and only if, $u_\theta = \Omega r$, where Ω is independent of r and z (rigid-body rotation). It follows that such a vortex represents a minimum energy state for the azimuthal velocity field, for a given angular momentum.

The angular velocity which gives rise to this minimum value of E_θ is

$$\Omega_0 = 2I_\Gamma/(R^2 V).$$

For an arbitrary velocity field u_θ, we may introduce an associated velocity $u'_\theta = u_\theta - \Omega_0 r$, where u'_θ is not, in general, small. Noting that u'_θ contains no net angular momentum, we may show that

$$E_\theta = \frac{I_\Gamma^2}{R^2 V} + \frac{1}{2}\int_V (u'_\theta)^2 \, \mathrm{d}V,$$

which is consistent with (13). The maximum kinetic energy which may be transferred between $\boldsymbol{u}_\theta$ and $\boldsymbol{u}_\mathrm{p}$ is therefore

$$\Delta E = \frac{1}{2}\int_V (u'_\theta)^2 \, \mathrm{d}V + E_\mathrm{p},$$

which is a constant for the flow.

Inertial waves may be superimposed, in a stable manner, on any z-independent swirl, $u_\theta = V(r)$, provided Rayleigh's discriminant is positive. For the particular case of $V(r) = \Omega r$, this follows directly from (13); that is, rigid-body rotation represents an *absolute* minimum in E_θ. More generally, it may be shown that any z-independent swirl, $u_\theta = V(r)$, in which Rayleigh's discriminant is positive, represents a *local* minimum in E_θ. This was shown by Moffatt (1986) and it is instructive to consider briefly his analysis.

Moffatt considers a virtual displacement field $\boldsymbol{\eta}(\boldsymbol{x})$, which satisfies $\boldsymbol{\nabla} \cdot \boldsymbol{\eta} = 0$ and $\boldsymbol{\eta} \cdot \mathrm{d}\boldsymbol{S} = 0$ on the boundary, but is otherwise arbitrary. This may be applied to any steady-state flow in such a way that the topology of the vortex lines is conserved. By this mechanism, we may consider all the possible velocity fields which are 'dynamically accessible' from the steady state by a small change in kinetic energy. We shall consider flows in which $\boldsymbol{\eta}(\boldsymbol{x})$ is not small in §5.

It is not difficult to show that, for the steady flow $u_\theta = V(r)$, the first- and second-order perturbations in velocity ($\delta^1\boldsymbol{u}$ and $\delta^2\boldsymbol{u}$) which preserve vortex line topology are

$$\delta^1 u_\theta = -\frac{1}{r}\Gamma'(r)\,\eta_r,$$

$$\delta^1 \boldsymbol{u}_\mathrm{p} = \frac{1}{r}\Gamma'(r)\,\eta_\theta \hat{\boldsymbol{e}}_r + \boldsymbol{\nabla}\phi,$$

$$\delta^2 u_\theta = \frac{1}{2r^2}\left[\frac{\partial}{\partial r}(r\Gamma'(r)\,\eta_r^2) + r\Gamma'(r)\frac{\partial}{\partial z}(\eta_z\,\eta_r)\right].$$

Note that these perturbation velocities ensure that $\delta^1 I_\Gamma$ and $\delta^2 I_\Gamma$ are both zero, so that angular momentum is conserved.

The perturbation in kinetic energy may be calculated from these expressions, and

it is clear that $\delta^1 E$ is zero (a necessary condition for $u_\theta = V(r)$ to be a steady state) while $\delta^2 E$ is given by

$$\delta^2 E = \delta^2 E_\theta + \delta^2 E_{\rm p} = \frac{1}{2}\int_V \Phi(r)\,\eta_r^2\,{\rm d}V + \frac{1}{2}\int_V (\delta^1 \boldsymbol{u}_{\rm p})^2\,{\rm d}V, \tag{14}$$

where $\Phi(r)$ is Rayleigh's discriminant.

Moffatt (1986) derived (14), but with the restriction that $\eta_\theta = 0$, so that $\delta^1 \boldsymbol{u}_{\rm p} = \boldsymbol{0}$ and $\delta^2 E_{\rm p}$ vanishes. It follows from this equation that the swirl flow $u_\theta = V(r)$ represents a local minimum in E_θ, provided $\Phi \geqslant 0$. Rayleigh's stability criterion also follows, since $\Phi \geqslant 0$ is a necessary and sufficient condition for E to be a local minimum.

If these perturbation velocities are substituted into (1) and (2), then we find that η_r satisfies the well-known inertial wave equation

$$\frac{\partial^2}{\partial t^2}\left\{\frac{\partial^2 \eta_r}{\partial z^2} + \frac{\partial}{\partial r}\left(\frac{1}{r}\frac{\partial}{\partial r}(r\eta_r)\right)\right\} + \Phi(r)\frac{\partial^2 \eta_r}{\partial z^2} = 0. \tag{15}$$

4.2. *The azimuthal vorticity and reversals in the recirculation*

Let $V_{\rm m}$ be an axisymmetric material volume, with surface $S_{\rm m}$ and bounding curve $C_{\rm m}$ in the (r,z)-plane. Equations (2) and (3) give

$$\frac{\rm D}{{\rm D}t}\int_{V_{\rm m}}\left(\frac{\omega_\theta}{r}\right){\rm d}V = \frac{\rm D}{{\rm D}t}\left\{2\pi\oint_{C_{\rm m}} \boldsymbol{u}_{\rm p}\cdot{\rm d}\boldsymbol{r}\right\} = \oint_{S_{\rm m}} \frac{\Gamma^2}{r^4}\hat{\boldsymbol{e}}_z\cdot{\rm d}\boldsymbol{S}. \tag{16}$$

Let us restrict ourselves to the case where the recirculation takes the form of a single poloidal eddy. Then we may use this equation to interpret the oscillatory behaviour seen in §3. If we take $V_{\rm m}$ to be V, the whole flow field, then the only contribution to the surface integral in (16) arises from the end faces of the cylinder. Now suppose that at time $t = 0$, Γ is larger on the face $z = 0$ than on $z = l$. In addition, suppose that $\boldsymbol{u}_{\rm p}$ is initially zero, as in the example in §3. Then (16) implies that a negative recirculation is produced, which will tend to advect the angular momentum on the end faces to the corners $(R,0)$ and $(0,l)$.

During this process $E_{\rm p}$, the kinetic energy of the recirculation, will increase in accordance with (12) since both ψ and $\partial u_\theta^2/\partial z$ are negative.

However, after one half of the 'reversal time', the excess angular momentum at $(0,l)$ will dominate the surface integral in (16), causing it to change sign. At this stage, the magnitude of ω_θ will start to decrease, and energy will be extracted from the poloidal velocity field since ψ and $\partial u_\theta^2/\partial z$ are then of opposite signs. Eventually, a positive value of ω_θ will be generated, changing the direction of the recirculation. The entire process is now reversed.

We shall develop an approximate, one-parameter model of this process in §5.

5. Characteristic times for the reversals in recirculation and for the diffusion on the axis

5.1. *Orders of magnitude*

We shall now examine more carefully velocity fields that are 'dynamically accessible' from the swirl flow $u_\theta = V(r)$, in the sense defined in §4.1. That is, velocity fields which have the same vortex line topology as $u_\theta = V(r)$, and are accessible from this flow by a finite perturbation in the kinetic energy. In particular, we shall look at the oscillatory advection of the swirl in the (r,z)-plane, as characterized by the distortion

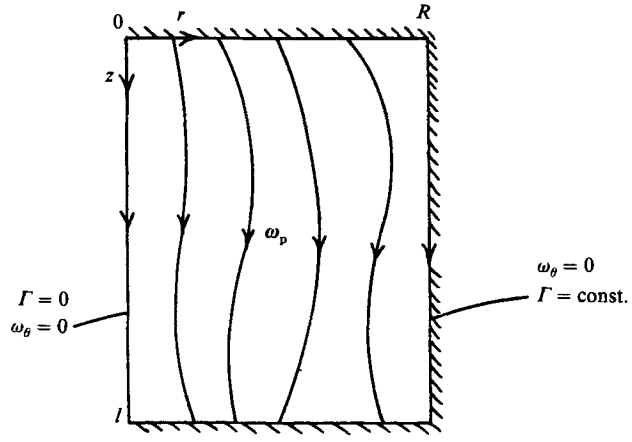

FIGURE 4. Necessary boundary conditions for a flow to be dynamically accessible from $u_\theta = V(r)$ by a change in kinetic energy only.

of the $\boldsymbol{\omega}_p$ lines. We may formally establish that the $\boldsymbol{\omega}_p$ lines are advected by $\boldsymbol{u}_p$ in the (r, z)-plane, by noting that Γ, the stream function for $\boldsymbol{\omega}_p$, is materially conserved.

We start by examining the restrictions that the initial boundary conditions place on the evolution of the flow. Consider a fluid particle which (initially) lies on the boundary. Its transverse velocity and acceleration are zero and it cannot pass through a stagnation point. Consequently, if it initially lies on an endwall, it must remain on that wall, and if it lies on the surface $r = R$, it must remain on that surface. Therefore, a poloidal vortex line which initially intersects with any of these surfaces, must continue to intersect with the same surface(s).

The flow $u_\theta = V(r)$ has parallel poloidal vortex lines ω_z, which intersect with the end faces $z = 0, l$. It follows that the only boundary conditions that are dynamically compatible with this flow (in the sense defined above) are ones in which all the poloidal vortex lines intersect with, and only with, these faces. Consequently, we must restrict ourselves to initial conditions in which $r = R$ is a poloidal vortex line, implying that Γ is constant along this surface. This angular momentum will then remain constant on $r = R$, equal to $\hat{\Gamma}$, for all $t > 0$.

This is not, however, the only initial boundary condition which the flow must satisfy. Since Γ is constant on $r = R$, (2) implies that $\mathrm{D}\omega_\theta/\mathrm{D}t = 0$ on this surface. But $\omega_\theta = 0$ in the flow $u_\theta = V(r)$, and consequently we require ω_θ to be zero on $r = R$ at time $t = 0$. Moreover, on the axis we have $\omega_\theta = 0$ (by symmetry) and $\Gamma = 0$ (for finite kinetic energy). These boundary conditions are illustrated in figure 4, which shows the initial distribution of the $\boldsymbol{\omega}_p$ lines. As the flow evolves, the volume enclosed between any two of these poloidal vortex lines remains constant.

It is interesting to note that the inertial waves and perturbation velocities discussed in §4.1. satisfy all these boundary conditions. These inertial waves give rise to a standing wave pattern in the poloidal vortex lines, which is illustrated in figure 5.

We shall now restrict attention to flows in which the recirculation consists of a single poloidal eddy. (Note, however, that even if the recirculation starts as a single eddy, it may subsequently break up into a number of smaller eddies.) When the azimuthal vorticity is positive, all the poloidal vortex lines on the end face $z = 0$ will tend to pile up on the axis, while all those on $z = l$ accumulate at the corner $r = R$.

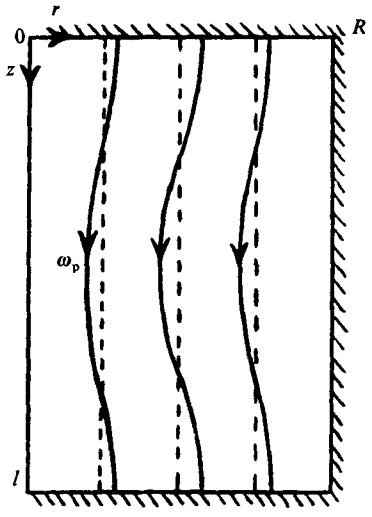

FIGURE 5. Inertial waves generate a standing wave pattern in the poloidal vortex lines ($E_p \ll E_\theta$).

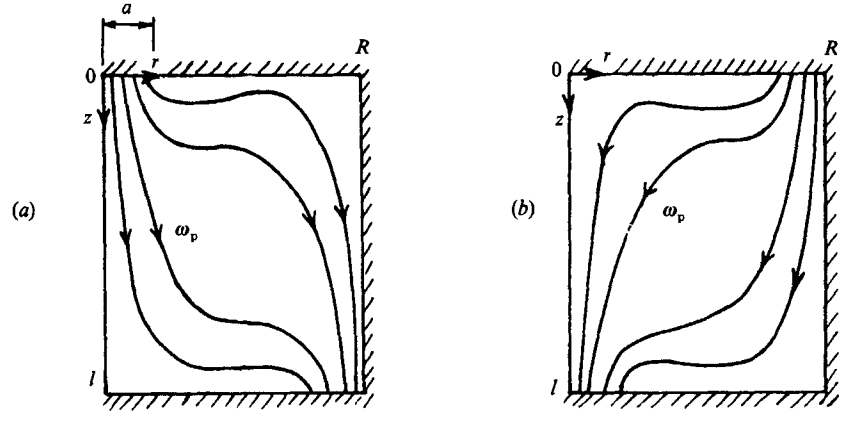

FIGURE 6. Accumulation of poloidal vortex lines in the corners ($E_p \sim E_\theta$): (a) $\omega_\theta > 0$, (b) $\omega_\theta < 0$.

Conversely, if ω_θ is negative, the vortex lines pile up at $(R, 0)$ and $(0, \overline{l})$. In either case, singularities start to form at the corners and on the axis. This is illustrated in figure 6.

However, in the short term, such singularities cannot develop because they are associated with an infinite kinetic energy on the axis. The mechanism by which they are avoided is as follows. Suppose that ω_θ is positive, so that the vortex lines start to pile up at $(0, 0)$ and (R, l). Then

$$\frac{\mathrm{d}}{\mathrm{d}t}\int_V \frac{\omega_\theta}{r}\mathrm{d}V = \oint_S \left(\frac{\Gamma^2}{r^4}\right)\hat{\boldsymbol{e}}_z \cdot \mathrm{d}\boldsymbol{S} < 0,$$

resulting in a reduction in ω_θ. The presence of the r^{-4} term in the surface integral ensures that this integral is dominated by the growing singularity at $(0, 0)$. As the vortex lines pile up in the corners, this integral will become large and negative. Eventually the flow will reverse, causing the vortex lines to move out of the corners $(0, 0)$ and (R, l), and into the opposite corners. Clearly, oscillations may develop in which the vortex lines alternately accumulate in opposite corners.

We might expect that the degree to which vortex lines accumulate in the corners will depend on the relative sizes of the swirl and recirculation. For example, suppose that there is a strong recirculation. Then we would expect that, before a reversal in ω_θ can occur, there must be a large concentration of poloidal vortex lines in the corners. In such a case a small but finite viscosity ν could cause appreciable diffusion.

We may estimate the extent to which the vortex lines pile up in the corners as follows. Suppose that (initially) ω_θ is positive, so that the vortex lines start to pile up at $(0,0)$ and (R,l). Let $\hat{E}_\mathrm{p}$ and $\hat{E}_\theta$ be the characteristic kinetic energies of $\boldsymbol{u}_\mathrm{p}$ and $\boldsymbol{u}_\theta$, and let a be the characteristic radius of the area (near $(0,0)$) into which the bulk of the vortex lines move. For simplicity, we shall take R and l to be of the same order.

There are three relevant timescales. Let τ_ν be the characteristic diffusion time in the corner $(0,0)$, and τ_r be the time taken for the recirculation to reverse, causing the vortex lines to move back out of the corners. The third characteristic time is the turn-over time of the poloidal eddy, τ_t, which is of order $\hat{\omega}_\theta^{-1}$.

We may relate the reversal time τ_r to a using (16):

$$\frac{\mathrm{d}}{\mathrm{d}t}\int_V \frac{\omega_\theta}{r}\,\mathrm{d}V = \oint_S \left(\frac{\Gamma^2}{r^4}\right)\hat{\boldsymbol{e}}_z\cdot\mathrm{d}\boldsymbol{S}.$$

The left-hand side of this equation is of order $\hat{\omega}_\theta R^2/\tau_\mathrm{r}$, while the right-hand side is dominated by the developing singularity at $(0,0)$, and is of order $\hat{\Gamma}^2/a^2$. Equating these two estimates, we obtain

$$\tau_\mathrm{r}\tau_\mathrm{t} \sim \frac{R^2a^2}{\hat{\Gamma}^2}. \tag{17}$$

We may also determine τ_r from the time taken for a fluid particle to move from an initial radius r_0 (of order R) to a radius of order a. That is,

$$\tau_\mathrm{r} \sim \int_a^{r_0}\frac{\mathrm{d}r}{u_r}, \quad u_r \sim -\hat{\omega}_\theta r,$$

from which,

$$\frac{\tau_\mathrm{r}}{\tau_\mathrm{t}} \sim \ln\left(\frac{R}{a}\right). \tag{18}$$

Eliminating τ_r from (17) and (18), and relating τ_t to $\hat{E}_\mathrm{p}$, gives

$$\left(\frac{R}{a}\right)^2\ln\left(\frac{R}{a}\right) \sim \frac{\hat{E}_\mathrm{p}}{\hat{E}_\theta}, \tag{19}$$

confirming that the extent to which the vortex lines accumulate on the axis depends on the relative strengths of the recirculation and the swirl. If $\hat{E}_\mathrm{p} \gg \hat{E}_\theta$, then a is much less than R.

The diffusion timescale τ_ν is of order a^2/ν, and so (17) gives

$$\frac{\tau_\nu}{\tau_\mathrm{r}} \sim \mathbb{R}\left(\frac{\hat{E}_\theta}{\hat{E}_\mathrm{p}}\right)^{\frac{1}{2}}, \tag{20}$$

where $\mathbb{R}$ is the Reynolds number $\hat{\Gamma}/\nu$. Whether or not diffusion has time to act depends on both $\mathbb{R}$ and the kinetic energy ratio $\hat{E}_\theta/\hat{E}_\mathrm{p}$. For an inviscid analysis to be applicable, we require $\tau_\nu \gg \tau_\mathrm{r}$. The stronger the recirculation (relative to the swirl),

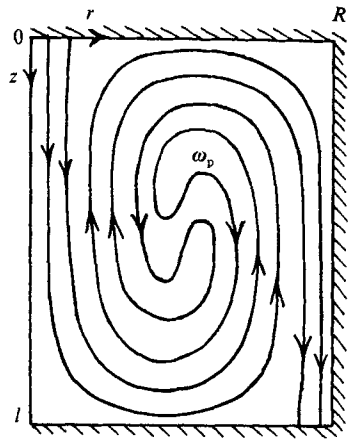

FIGURE 7. Spiralling of the poloidal vortex lines by the recirculation ($E_p \gg E_\theta$).

the more pronounced is the pile-up of vortex lines at the corners, and the greater the likelihood of appreciable diffusion. Equation (20) may be rewritten as

$$\tau_\nu \sim \frac{R^2}{\nu}\left(\frac{\hat{\Gamma}\tau_t}{R^2}\right)^2 \left|\ln\left(\frac{\hat{\Gamma}\tau_t}{R^2}\right)\right|,$$

which was the equation used in §1 to characterize the diffusion timescale for a concentrated vortex core on the axis.

Note that (18) implies that, if $\hat{E}_p \gg \hat{E}_\theta$ (so that $a \ll R$), then the turn-over time will be much less than τ_r. Consequently, if the initial recirculation is strong, a poloidal eddy will 'turn over' many times before the recirculation reverses direction. In such a situation we would expect that the poloidal vortex lines will become highly spiralled and convoluted in the core of the flow. This is illustrated in figure 7. On the other hand, if $\hat{E}_p \sim \hat{E}_\theta$ (so that $a \sim R$), then the turn-over time is of the same order as τ_r, and we would not expect the same degree of stretching and twisting of the vortex lines. In this case a situation similar to that shown in figure 6 may develop.

From the discussion above it is clear that we may categorize the initial development of the flow according to the relative sizes of $\hat{E}_p$ and $\hat{E}_\theta$.

(*a*) $\hat{E}_p \ll \hat{E}_\theta$ (strong swirl case; figure 5). Here we have standing waves superimposed on parallel poloidal vortex lines. There is no tendency for poloidal vortex lines to accumulate in the corners.

(*b*) $\hat{E}_p \sim \hat{E}_\theta$ (swirl and recirculation of comparable size; figure 6). In this case the poloidal vortex lines do accumulate in the corners, although the characteristic radius into which the bulk of the vortex lines move, a, is a significant fraction of R. Reversals of the recirculation will occur in a time τ_r which is of the same order as the turn-over time τ_t.

(*c*) $\hat{E}_p \gg \hat{E}_\theta$ (strong initial poloidal flow; figure 7). The poloidal vortex lines pile up in corner regions of characteristic radius a, which is much less than R. Also, the reversal time τ_r is longer than the turn-over time, so that the vortex lines become stretched and convoluted. The diffusion time τ_ν is reduced owing to the pile-up of the vortex lines, while the increase in spatial gradients in the interior may lead to Prandtl–Batchelor homogenization, which would tend to dampen any oscillations.

We shall now quantify these estimates with an approximate one-parameter model of the oscillations.

5.2. *A simple, one-parameter model of nonlinear oscillations*

Let us consider the idealized situation where the poloidal recirculation takes the form of a single eddy and, although its magnitude varies with time, its spatial distribution remains approximately constant. The stream function is even in r and zero on the boundary, so perhaps the simplest approximation for ψ is

$$\psi = A(t)\left\{\frac{lR}{\pi}\left(\frac{r}{R}\right)^2\left[1-\left(\frac{r}{R}\right)^2\right]\sin\left(\frac{\pi z}{l}\right)\right\}, \tag{21}$$

where $A(t)$ is an unknown amplitude. We shall derive a differential equation for $A(t)$ using (16), which we may rewrite as

$$\frac{\mathrm{d}}{\mathrm{d}t}\oint_C \boldsymbol{u}_\mathrm{p}\cdot\mathrm{d}\boldsymbol{r} = \int_{\substack{0\\z=l}}^{R}\frac{\Gamma^2}{r^3}\mathrm{d}r - \int_{\substack{0\\z=0}}^{R}\frac{\Gamma^2}{r^3}\mathrm{d}r. \tag{22}$$

We start by converting the right-hand side of this equation into an expression involving only $A(t)$ and the initial conditions. We do this by considering the history of fluid particles on the endwalls. Equation (21) gives

$$u_r = -A(t)\left\{\left(\frac{r}{R}\right)\left[1-\left(\frac{r}{R}\right)^2\right]\cos\left(\frac{\pi z}{l}\right)\right\}.$$

Now consider a fluid particle which lies on the endwall $z = l$. Let its instantaneous position be $r_p(t)$ and its initial position be r_0. Then we may integrate this expression for u_r, following the fluid particle, to give

$$\frac{R^2-r_p^2}{r_p^2} = \frac{R^2-r_0^2}{r_0^2}\exp\left[-\frac{2}{R}\int_0^t A(t)\,\mathrm{d}t\right].$$

As the particle moves, it conserves its angular momentum Γ, and so

$$\frac{\Gamma_p^2\,\delta r_p}{r_p^3} = \frac{\Gamma_0^2\,\delta r_0}{r_0^3}\exp\left[-\frac{2}{R}\int_0^t A(t)\,\mathrm{d}t\right],$$

from which, on the endwall $z = l$, we have

$$\int_0^R \frac{\Gamma^2}{r^3}\mathrm{d}r = \left[\int_0^R \frac{\Gamma^2}{r^3}\mathrm{d}r\right]_{t=0}\exp\left[-\frac{2}{R}\int_0^t A(t)\,\mathrm{d}t\right].$$

We may now substitute for the integrals on the right-hand side of (22). For convenience, we introduce the following constants which are determined by the initial swirl distribution:

$$\Omega_l^2 = \frac{2}{R^2}\int_0^R \frac{\Gamma^2}{r^3}\mathrm{d}r; \quad z = l, \quad t = 0,$$

$$\Omega_0^2 = \frac{2}{R^2}\int_0^R \frac{\Gamma^2}{r^3}\mathrm{d}r; \quad z = 0, \quad t = 0.$$

Then, evaluating $\oint \boldsymbol{u}_\mathrm{p}\cdot\mathrm{d}\boldsymbol{r}$ using (21), and substituting for the angular momentum integrals using the expressions above, we obtain the following integro-differential equation:

$$\frac{\kappa}{R}\dot{A}(t) = \Omega_l^2\exp\left[-\frac{2}{R}\int_0^t A(t)\,\mathrm{d}t\right] - \Omega_0^2\exp\left[+\frac{2}{R}\int_0^t A(t)\,\mathrm{d}t\right], \tag{23}$$

where κ is the constant $\kappa = 1+\left(\frac{4l}{\pi R}\right)^2$.

This equation involves only the unknown amplitude $A(t)$ and the initial conditions, as specified by Ω_l and Ω_0. Moreover, it is not restricted to cases where the initial swirl is in a state of (almost) rigid-body rotation. For simplicity, we shall consider now the symmetric case, in which $\Omega_l = \Omega_0$. Then (23) simplifies to

$$\frac{\kappa}{2R}\dot{A}(t) = -\Omega_0^2 \sinh\left[\frac{2}{R}\int_0^t A(t)\,\mathrm{d}t\right]. \tag{24}$$

This represents a mass–spring system with a restoring force proportional to $\Omega_0^2 \sinh(x)$, where x is a displacement.

For small-amplitude oscillations, (24) may be linearized to give

$$\ddot{A}(t)+\frac{4\Omega_0^2}{\kappa}A(t) = 0,$$

with an associated natural frequency of

$$\omega_n = \frac{2\Omega_0}{[1+(4l/\pi R)^2]^{\frac{1}{2}}}. \tag{25}$$

For the particular case of rigid-body rotation, we may compare this with the exact solution for standing inertial waves in a cylinder. Analysis of (5) shows that the fundamental mode, to which our analysis corresponds, has a natural frequency of

$$\omega_n = \frac{2\Omega}{[1+(\delta_1 l/\pi R)^2]^{\frac{1}{2}}}, \quad \delta_1 = 3.83$$

which is very close to the approximate expression (25). (This frequency would be predicted exactly if the assumed function of radius in (21) corresponded to the fundamental mode for inertial waves.)

We now integrate (24) to give a first-order equation. Noting that A has the dimensions of a velocity, we let V_0 be the initial value of A. Then

$$\tfrac{1}{2}A^2(t)-\tfrac{1}{2}V_0^2 = -\frac{\Omega_0^2 R^2}{\kappa}\left\{\cosh\left[\frac{2}{R}\int_0^t A(t)\,\mathrm{d}t\right]-1\right\},$$

which could be integrated numerically to give $A(t)$. However, the reversal time τ_r may be estimated directly from this expression by putting $A(t) = 0$, giving

$$V_0^2 \sim \Omega_0^2 R^2\left\{\cosh\left[\frac{V_0\tau_r}{R}\right]-1\right\}.$$

For small-amplitude oscillations (in the sense that $V_0 \ll \Omega_0 R$) this gives us $\tau_r \sim \Omega_0^{-1}$, which is consistent with (25). For large-amplitude oscillations, in which $V_0 \gg R/\tau_r$, we obtain

$$\tau_r \sim \frac{R}{V_0}\ln\left(\frac{V_0}{\Omega_0 R}\right),$$

which is consistent with (18) and (19).

Figures 8(*a*) and 8(*b*) compare the analytical model with the results of the numerical experiments described in §3. In particular, they show the predicted variation in the maximum poloidal velocity, obtained by integrating (23). It can be seen that the model tends to overestimate the period of oscillation by up to 4%,

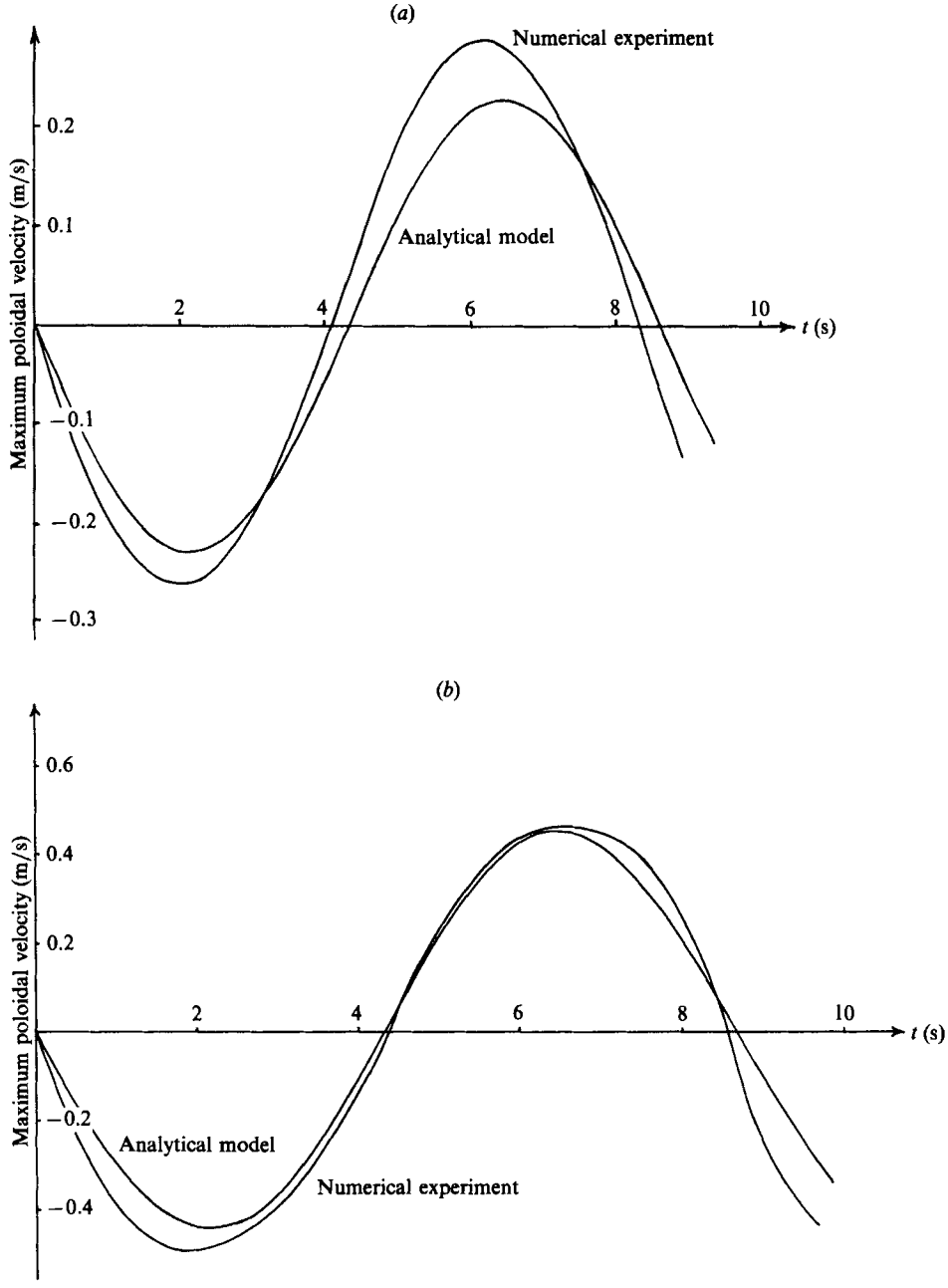

FIGURE 8. Comparison of the approximate analytical model with the numerical experiment described in §3. (*a*) Initial conditions given by (6); (*b*) initial conditions given by (7).

while underestimating the size of the recirculation, by up to 20%. This error in estimating the magnitude of the recirculation is primarily a consequence of having assumed a simple shape function for ψ.

In addition to the comparison above, it would be instructive to compare the model with laboratory experiments, such as those of Kojima *et al.* (1983). Unfortunately, there is insufficient data given in that paper to afford such a comparison.

Thus we have a simple, one-parameter model for finite-amplitude oscillations in a cylinder. Of course, such an analysis is valid only for as long as the recirculation remains in the form of a single eddy, and even within this time period, the assumption that ψ can be represented by (21) is a severe restriction. Nonetheless, it gives some insight into what occurs in the initial stages of the flow.

6. Flows in which the swirl is zero on the boundary

We shall now consider briefly flows in which Γ is zero on the boundary S. Although such flows will not, in general, exhibit oscillatory behaviour, they are of some interest because they possess a number of integral invariants.

Note that, for Γ to be zero on S, for all $t > 0$, it is only necessary that Γ be zero on S at $t = 0$. This follows from the fact that Γ is materially conserved, and that fluid particles initially lying on S, remain on S.

Since the angular momentum Γ is the stream function for the poloidal vorticity, the boundary condition $\Gamma = 0$ implies that the vortex lines are closed within the fluid. Let C_Γ be a closed poloidal vortex line, defined by $\Gamma = \Gamma_0$, and let V_Γ be the toroidal volume enclosed by C_Γ. This is illustrated in figure 9. We shall examine a number of integral invariants associated with the volume V_Γ. The first thing to note is that V_Γ is itself conserved, so that the function $V_\Gamma(\Gamma)$, the variation of enclosed volume with Γ, remains constant as the flow evolves.

Each volume V_Γ possesses a number of integrals which are constant for purely kinematic reasons. For example, the integrals of ω_r and ω_z throughout V_Γ are both zero. More generally, the moments of vorticity are zero (see Truesdell & Toupin 1960). However, we shall be concerned here with dynamic invariants.

From the equations of motion (1) and (2) we may deduce

$$\frac{\mathrm{D}}{\mathrm{D}t}\left(g(\Gamma)\frac{\omega_\theta}{r}+f(\Gamma)\right) = \nabla\cdot\left(\frac{2}{r^4}\int_0^\Gamma \Gamma g(\Gamma)\,\mathrm{d}\Gamma\,\hat{\boldsymbol{e}}_z\right).$$

Integrating this equation throughout V_Γ, invoking the divergence theorem, and noting that Γ is constant on C_Γ, we may show that there is a general invariant of the form

$$\frac{\mathrm{d}}{\mathrm{d}t}\int_{V_\Gamma}\left[g(\Gamma)\frac{\omega_\theta}{r}+f(\Gamma)\right]\mathrm{d}V = 0, \tag{26}$$

where g and f are arbitrary functions of Γ. We shall consider three particular forms of (26).

If we take $g = 1$ and $f = 0$, then we obtain

$$\frac{\mathrm{d}}{\mathrm{d}t}\oint_{C_\Gamma}\boldsymbol{u}_\mathrm{p}\cdot\mathrm{d}\boldsymbol{r} = 0, \tag{27}$$

so that the circulation in the (r, z)-plane, around C_Γ, remains constant. (Note that this is not merely a restatement of Kelvin's circulation theorem, since this line integral remains in the (r, z)-plane, there being no contribution from u_θ.) If $\boldsymbol{u}_\mathrm{p}$ is initially zero, this implies that the recirculation cannot take the form of a single eddy.

If we now take $g(\Gamma) = \Gamma$ and $f = 0$, then (26) gives us

$$\frac{\mathrm{D}}{\mathrm{D}t}\int_{V_\Gamma} u_\theta\omega_\theta\,\mathrm{d}V = 0. \tag{28}$$

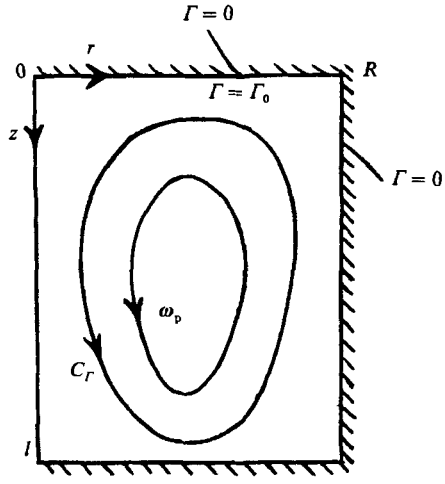

FIGURE 9. Flow in which the angular momentum is zero on the boundary.

This is reminiscent of the helicity integral

$$H = \int_{V_\Gamma} \boldsymbol{u} \cdot \boldsymbol{\omega} \, \mathrm{d}V,$$

which may be shown to be constant (Moffatt 1978). Let us divide H into two components, H_θ and H_p, defined by

$$H_\theta = \int_{V_\Gamma} u_\theta \omega_\theta \, \mathrm{d}V, \quad H_\mathrm{p} = \int_{V_\Gamma} \boldsymbol{u}_\mathrm{p} \cdot \boldsymbol{\omega}_\mathrm{p} \, \mathrm{d}V.$$

Then (28) gives

$$\frac{\mathrm{d}H}{\mathrm{d}t} = \frac{\mathrm{d}H_\theta}{\mathrm{d}t} = \frac{\mathrm{d}H_\mathrm{p}}{\mathrm{d}t} = 0. \tag{29}$$

The invariance of H_θ and H_p is, in fact, a direct consequence of (27), combined with the conservation of helicity. This may be shown by integrating the identity

$$\nabla \cdot (\boldsymbol{u}_\theta \times \boldsymbol{u}_\mathrm{p}) = \boldsymbol{u}_\mathrm{p} \cdot \boldsymbol{\omega}_\mathrm{p} - \boldsymbol{u}_\theta \cdot \boldsymbol{\omega}_\theta$$

to give

$$H_\theta = \tfrac{1}{2}H + \pi\Gamma_0 \oint_{C_\Gamma} \boldsymbol{u}_\mathrm{p} \cdot \mathrm{d}\boldsymbol{r}, \tag{30}$$

$$H_\mathrm{p} = \tfrac{1}{2}H - \pi\Gamma_0 \oint_{C_\Gamma} \boldsymbol{u}_\mathrm{p} \cdot \mathrm{d}\boldsymbol{r}. \tag{31}$$

Conservation of H_θ and H_p gives rise to further restrictions on the flow. For example, if we apply the Schwarz inequality to the integrals H_θ and H_p, taken throughout the flow field, then we obtain the following lower bounds for the components of enstrophy:

$$\int_V \omega_\theta^2 \, \mathrm{d}V \geqslant \frac{H^2}{8E_\theta} \geqslant \frac{H^2}{8E}, \quad \int_V \omega_\mathrm{p}^2 \, \mathrm{d}V \geqslant \frac{H^2}{8E_\mathrm{p}} \geqslant \frac{H^2}{8E}.$$

The third form of (26) that we shall examine concerns only the swirl. If we take $g = 0$ and $f = \Gamma$, then we see that angular momentum is conserved in V_Γ. Let $\boldsymbol{x}$ be the

position vector $(r, 0, z)$. Then, by expanding the axial component of $\boldsymbol{x} \times (\boldsymbol{x} \times \boldsymbol{\omega})$ to give $-\boldsymbol{x} \cdot \nabla \Gamma$, we obtain the invariant

$$\frac{1}{3}\int_{V_\Gamma} \boldsymbol{x} \times (\boldsymbol{x} \times \boldsymbol{\omega})\, \mathrm{d}V = \left[\int_{V_\Gamma} \Gamma \mathrm{d}V - \Gamma_0 V_\Gamma\right] \hat{\boldsymbol{e}}_z. \tag{32}$$

When $V_\Gamma = V$, the entire flow field, this expression takes on the familiar form of the torque required to initiate the motion (Batchelor 1967). Equation (32) provides an additional lower bound on the enstrophy of the swirl. Applying the Schwarz inequality, we may show that

$$\int_V \omega_{\mathrm{p}}^2 \, \mathrm{d}V \geqslant \frac{54 I_\Gamma^2}{R^2(l^2 + 2R^2)\, V}.$$

Thus, flows in which Γ is initially zero on the boundary possess a number of invariants, most of which may be derived from the general form given in (26). In association with the conservation of energy, these place significant restrictions on the manner in which the flow may evolve.

It may be noted that there is at least one steady-state solution of the equations of motion which satisfies $\Gamma = 0$ on the boundary. This is

$$\psi = A r J_1(\delta_n r/R) \sin(m\pi z/l), \quad \Gamma = a\psi,$$

where $a^2 = (\delta_n/R)^2 + (m\pi/l)^2$.

This is a Beltrami flow with $\boldsymbol{\omega} = a\boldsymbol{u}$ and is, in fact, the only possible axisymmetric Beltrami flow in a cylinder. However, such a flow could not be realized in practice, as viscosity determines the steady state.

7. Conclusions

In general, an initially non-uniform swirl distribution gives rise to a strong, oscillatory recirculation. Energy is exchanged between the swirl and the recirculation, the direction of transfer depending on the relative signs of ψ and $\partial u_\theta/\partial z$. Conservation of angular momentum imposes a limit on the amount of transferable energy, by creating a lower bound for the kinetic energy of the swirl.

When the poloidal vortex lines intersect the endwalls, there is a tendency for the vortex lines to accumulate at the corners and on the axis. This is particularly the case when the swirl is weak, and leads to accelerated local diffusion on the axis.

An elementary, one-parameter model is proposed for the nonlinear oscillations. This predicts that the flow behaves like a mass–spring system with a nonlinear restoring force proportional to $\Omega_0^2 \sinh(x)$, where x is a displacement. This allows estimates to be made of the reversal time for the recirculation.

When the swirl is initially zero on the boundary, the flow possesses the general integral invariant

$$\int_{V_\Gamma} \left[g(\Gamma)\frac{\omega_\theta}{r} + f(\Gamma)\right] \mathrm{d}V,$$

where g and f are arbitrary functions of Γ, and V_Γ is the volume enclosed by a poloidal vortex line C_Γ. This, in turn, implies the constancy of the helicity-like integrals H_θ and H_{p} and of the circulation, $\oint_{C_\Gamma} \boldsymbol{u}_{\mathrm{p}} \cdot \mathrm{d}\boldsymbol{r}$.

The author is grateful to A. J. Mestel for some useful comments on the original manuscript and to F. Boysan for his assistance with the computations.

REFERENCES

BATCHELOR, G. K. 1951 Note on a class of solutions of the Navier–Stokes equations representing steady rotationally-symmetric flow. *Q. J. Mech. Appl. Maths* **IV**, 29–41.

BATCHELOR, G. K. 1956 On steady laminar flow with closed streamlines at large Reynolds number. *J. Fluid Mech.* **1**, 177–190.

BATCHELOR, G. K. 1967 *An Introduction to Fluid Mechanics*. Cambridge University Press.

BLOOR, M. I. G. & INGHAM, D. B. 1987 The flow in industrial cyclones. *J. Fluid Mech.* **178**, 507–519.

DAVIDSON, P. A. & HUNT, J. C. R. 1987 Swirling, recirculating flow in a liquid metal column generated by a rotating magnetic field. *J. Fluid Mech.* **185**, 67–106.

DIJKSTRA, D. & HEIJST, G. J. F. VAN 1983 The flow between two finite rotating discs enclosed by a cylinder. *J. Fluid Mech.* **128**, 123–154.

DRAZIN, P. G. & REID, W. H. 1981 *Hydrodyanic Stability*, pp. 77–80. Cambridge University Press.

GREENSPAN, H. P. 1968 *The Theory of Rotating Fluids*. Cambridge University Press.

GUPTA, A. K., LILLEY, D. G. & SYRED, N. 1984 *Swirl Flows*. Energy and Engineering Science Series, Abacus Press.

HALL, M. G. 1967 The structure of concentrated vortex cores. *Prog. Aeronaut. Sci.* **7**, 53–110.

HOWARD, L. N. & GUPTA, A. S. 1962 On the hydrodynamic and hydromagnetic stability of swirling flows. *J. Fluid Mech.* **14**, 463–476.

KOJIMA, S., OHNISHI, T., MORI, T., SHIWAKU, K., WAKASUGI, I. & OHGAMI, M. 1983 Application of advanced mild stirring to a new bloom caster; the latest Kosmostir-Magnetogyr process technique. *Proc. 66th Steelmaking Conf., Atlanta, USA, Iron and Steel Soc. of AIME.*

LEWELLEN, W. S. 1962 A solution for three-dimensional vortex flows with strong circulation. *J. Fluid Mech.* **14**, 420–432.

MOFFATT, H. K. 1978 *Magnetic Field Generation in Electrically Conducting Fluids*, pp. 14–47. Cambridge University Press.

MOFFATT, H. K. 1986 Magnetostatic equilibria and analogous Euler flows of arbitrarily complex topology. Part 2. Stability considerations. *J. Fluid Mech.* **166**, 359–378.

TRUESDELL, C. & TOUPIN, R. 1960 The classical field theories. In *Handbuch der Physik*, Band III/1 (ed. S. Flügge), pp. 226–793. Springer.